TRANSACTIONS ON ELECTRICAL AND ELECTRONIC MATERIALS
Vol. 18, No. 4, pp. 221-224, August 25, 2017

Regular Paper

pISSN: 1229-7607 eISSN: 2092-7592
DOI: https://doi.org/10.4313/TEEM.2017.18.4.221
OAK Central: http://central.oak.go.kr

Extraction of Series Arc Signals Based on Wavelet Transform in an Indoor Wiring System

Hong-Keun Ji and Young-Jin Cho
National Forensic Service Busan Institute, Forensic Safety Section, Yangsan 50612, Korea

Guoming Wang, Seong-Cheol Hwang, and Gyung-Suk Kil†
Department of Electrical and Electronics Engineering, Korea Maritime and Ocean University, Busan 49112, Korea

Received January 21, 2017; Revised June 5, 2017; Accepted June 8, 2017

This paper dealt with the extraction of series arc signals based on wavelet transform in order to improve the accuracy of arc detection in indoor wiring systems. Three types of arc sources including a cord-cord, a terminal-cord, and an outlet-plug were fabricated to simulate typical arc defects. An arc generator fabricated according to UL 1699 was used to generate arcs. The optimal mother wavelet was selected as bior1.5 by calculating the correlation coefficients between the detected single current pulse and the wavelet. The detected arc current signals were then decomposed into eight levels using the discrete wavelet transform that implements the multi-resolution analysis method. By analyzing the decomposed components, the detail components D6, D7, and D8 were associated with arc signals, which were used for signal reconstruction. From the result, it was verified that the proposed method can be used for the extraction of the series arc signal from the AC mains, which is expected to be applied to further analysis of arc signals in indoor wiring systems.

Keywords : Series arc, Indoor wiring system, Wavelet transform, Multi-resolution analysis, Decomposition

1. INTRODUCTION

Electrical arc is defined as a luminous discharge of electricity across an insulating medium, usually accompanied by the partial volatilization of the electrodes [1]. Arc faults can be generated from a loose connections between conductors or a breakdown of the insulation. As a result, a carbonized path between the two electrodes may be formed thereby leading to electrical fires [2-4].

According to the statistical analysis provided by the National Fire Data System, 8,873 electrical fires occurred in Korea in 2016, which accounted for 20.6% of all fire accidents, resulting in enormous economic losses and human injuries. Therefore, it is essential to detect arc signals in advance in order to prevent electrical fires.

Although circuit breakers are installed in residential branch circuits for overcurrent protection, there are regions where no operation is activated to protect against the effects of arcs [5,6]. The arc-fault circuit interrupter (AFCI) is intended to provide protection from the effects of arc faults by recognizing the characteristics unique to arcing and by de-energizing the circuit when an arc fault is detected [1,6,7]. However, arc faults are usually superposed on the AC mains when detected by a current transformer, and it is difficult to distinguish the minute arc events.

The wavelet transform (WT), which analyzes a signal in the time and frequency domains simultaneously, has achieved its wide application in the field of signal processing, including the feature extraction and signal de-nosing [8-12]. Therefore, in this paper, a method is proposed for extraction of series arc signals from the AC mains using the WT technique for accurate detection of arcs in indoor wiring systems. The optimal mother wavelet was selected. The arc signals were reconstructed using only those components that were related to the arcing fault.

† Author to whom all correspondence should be addressed:
E-mail: kilgs@kmou.ac.kr

2. EXPERIMENTS

Figure 1 shows the sources of electrical fires investigated by the National Forensic Service, which were caused by series arcs in indoor wiring systems. These accidents mainly resulted from loose connections between cords, between terminals and cords, and between outlets and plugs.

To simulate the real arc sources in an interior wiring system, three types of defects including a cord-cord, a terminal-cord, and an outlet-plug were fabricated, which are shown in Fig. 2. The cord-cord defect was used to simulate a frayed conductor in a cord or damage to the insulation. The poor connection between Y terminal and cord was simulated using the terminal-cord. The outlet-plug was fabricated to represent a worn-out outlet or a loose connection between outlet and plug.

The experimental setup is shown in Fig. 3. A 220 V AC mains and an arc generator were connected in series with a load. The arc generator designed according to UL 6199 consisted of a stationary and a moving electrode, which were used to fix the simulated arc source. The lateral adjustment was used to control the distance between the two electrodes such that current can flow in this circuit. A vibration motor was installed to excite the generation of arc. An adjustable load resistor was used as the load. The arc current signals were detected by a high-frequency current transformer (HFCT) with a frequency range up to 20 MHz and acquired using a digital storage oscilloscope (DSO) and a data acquisition (DAQ) unit. A WT analysis program was developed based on LabVIEW.

Unlike the Fourier transform, which only analyzes a signal in the frequency domain, the WT characterizes the signal in time and frequency domains simultaneously [8-10]. The continuous wavelet transform (CWT) is described by

Fig. 1. Suspected causes of electrical fires due to series arc.

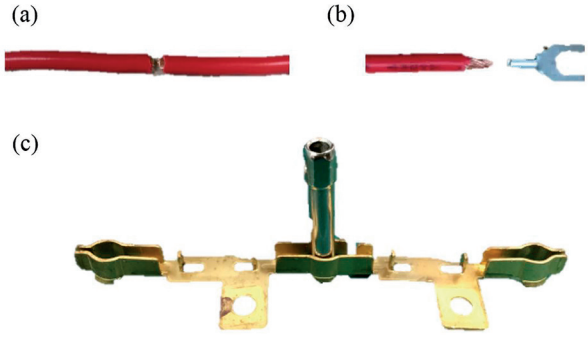

Fig. 2. Arc sources. (a) Cord-cord, (b) terminal-cord, and (c) outlet- plug.

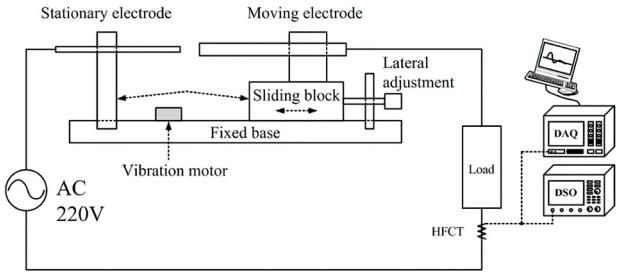

Fig. 3. Experimental setup.

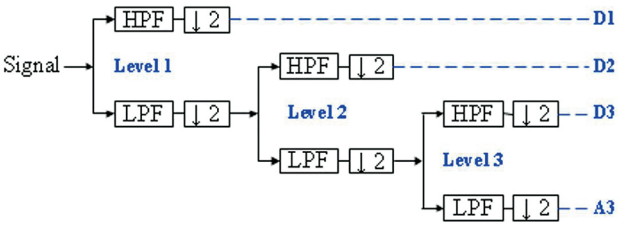

Fig. 4. Decomposition of a signal into three levels using MRA.

$$CWT_{\psi}f(a,b) = |a|^{-1/2}\int f(t)\Psi(\frac{t-b}{a})dt \quad (1)$$

where *f(t)* is the given signal, *ψ(t)* is the mother wavelet, and *a* and *b* are the scale and shift factors, respectively. Therefore, the WT decomposes the signal using the scaled and shifted versions of the mother wavelet. However, the CWT calculates the wavelet coefficients at every instant, resulting in excessive redundancy and intensive computation. As a result, the discrete wavelet transform (DWT) is used, which is implemented using the multi-resolution analysis (MRA). As shown in Fig. 4, which demonstrates decomposition of a signal into three levels, the signal is first down-sampled by a high pass filter (HPF) and a low pass filter (LPF), generating the detail (D) and approximation (A) coefficients, respectively. Then, the approximation component is passed through another level of filters using down-sampling. The decomposition continues until reaching the maximum decomposition level [11-16].

In this paper, the series arc current signal superposed on the AC mains was decomposed, and the components related to the arc signal were retained whereas those associated with the background signal were discarded. Finally, the signal was reconstructed with the retained components using the inverse DWT.

3. RESULTS AND DISCUSSIONS

3.1 Mother wavelet

Since the WT decomposes a signal into a family of a wavelet, a proper mother wavelet is important for improving the accuracy of signal processing. Among various types of mother wavelets, the biorthogonal (bior) has the linear-phase characteristic, meaning that it maintains a constant time delay for different frequencies, which makes it suitable for feature extraction [9]. To select the optimal mother wavelet, the correlation coefficient (CC) is used to compare the similarity between the detected single arc pulse and the wavelet. The CC is given by

$$CC = \frac{\sum_{i=1}^{N-1}[X(i)-\bar{X}][Y(i)-\bar{Y}]}{\sqrt{\sum_{i=1}^{N-1}[X(i)-\bar{X}]^2 \cdot \sum_{i=1}^{N-1}[Y(i)-\bar{Y}]^2}} \quad (2)$$

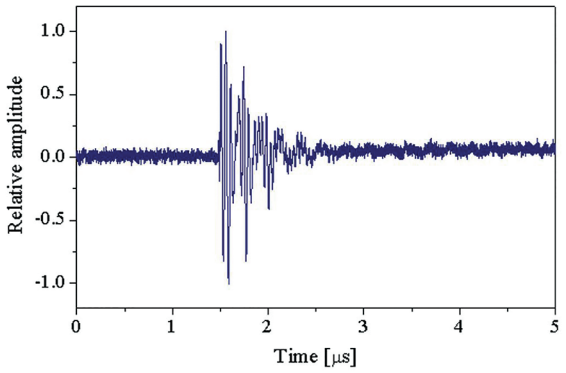

Fig. 5. Example of single arc pulse detected in the cord-cord fault.

Table 1. Correlation coefficient values between bior wavelets and single arc pulses.

Wavelet	Cord-cord	Terminal-cord	Outlet-plug
bior1.3	0.033	0.029	0.031
bior1.5	0.062	0.057	0.072
bior2.2	0.051	0.044	0.046
bior2.4	0.020	0.016	0.015
bior2.6	0.032	0.027	0.023
bior2.8	0.035	0.033	0.029
bior3.1	0.029	0.026	0.027
bior3.3	0.021	0.019	0.022
bior3.5	0.005	0.002	0.000
bior3.7	0.008	0.006	0.004
bior3.9	0.009	0.009	0.008

where *X(i)* and *Y(i)* are the single arc pulse and the mother wavelet, respectively, and $\bar{X}$ and $\bar{Y}$ are their mean values. A larger value of correlation coefficient indicates a greater similarity between these two signals [17,18].

Figure 5 shows an example of a single arc current pulse detected in the cord-cord defect. These pulses detected in three types of faults were used to select the optimal mother wavelet. Table 1 shows the CC values between the arc pulses and the biorthogonal wavelet. The number listed in the name of the wavelet indicates the order of the wavelet in its family. It is revealed that the bior1.5 had the highest similarity with arc pulses in all three types of arc sources. Therefore, bior1.5 was selected as the optimal wavelet.

3.2 Extraction of arc signals

After selecting the optimal mother wavelet, arc signals detected from three types of defects were decomposed into eight levels using the bior1.5. The sampling rate of signal acquisition was 1.25 MS/s, therefore, the highest frequency of detected signal was 625 kHz. The corresponding frequency bands of each component are listed in Table 2, which verifies that the MRA interprets the decomposed components into a series of independent frequency bands by applying the down-sampling method. In Table 2, components D1~D8 and A8 are the final result of MRA analysis whereas A1-A7 are the intermediate processes.

Figure 6 shows the extraction of the arc signal from the cord-cord fault, overlapped with the applied current waveform. In Fig. 6(a), six cycles of the mains current were measured and minute arc signals can be observed in the last three cycles. In addition, there were shoulders near the zero-crossing region of the mains current, which occurred as the arc was extinguished when the voltage dropped below the value required for sustaining the discharge. The detected signal was decomposed into eight levels using the bior1.5 mother wavelet. Fig. 6(b) shows that the approximation component A8 at

Table 2. Frequency bands of components at each level.

Level	Frequency (kHz)	
	Approximation (A)	Detail (D)
1	0-312.5	312.5-625
2	0-156.25	156.25-312.5
3	0-78.125	78.125-156.25
4	0-39.0625	39.0625-78.125
5	0-19.53125	19.53125-39.0625
6	0-9.765625	9.765625-19.53125
7	0-4.8828125	4.8828125-9.765625
8	0-2.44140625	2.44140625-4.8828125

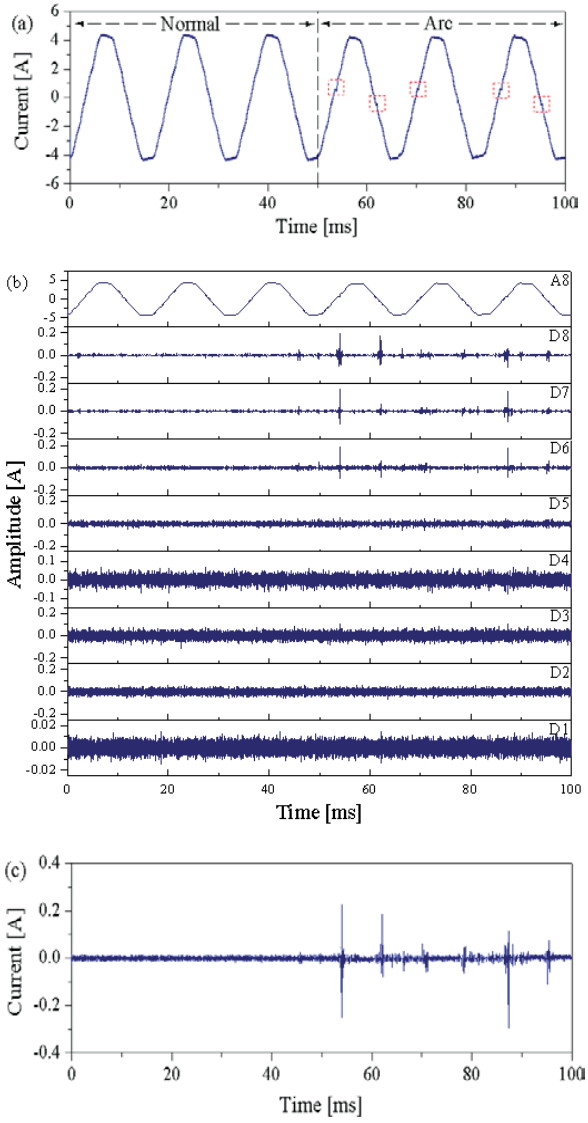

Fig. 6. Extraction of arc signal from the cord-cord fault. (a) Mains current, (b) decomposition of detected signal into eight levels, and (c) signal reconstructed using D6, D7, and D8.

the eighth level contained information regarding the mains current, and the detail components from D1 to D5 were associated with background noise. The series arc signals were identified in the detail components in levels 6, 7, and 8, which covered a frequency band of 2.44 kHz~19.53 kHz. Therefore, detail components D6, D7, and D8 were used for reconstructing the arc signal and the reconstructed signal is shown in Fig. 6(c).

To confirm the validity of the proposed method, the arc signals

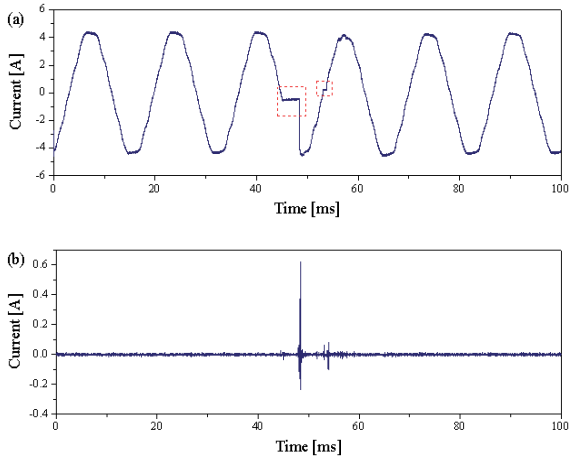

Fig. 7. Extraction of arc signal from the terminal-cord fault. (a) Mains current and (b) signal reconstructed using D6, D7, and D8.

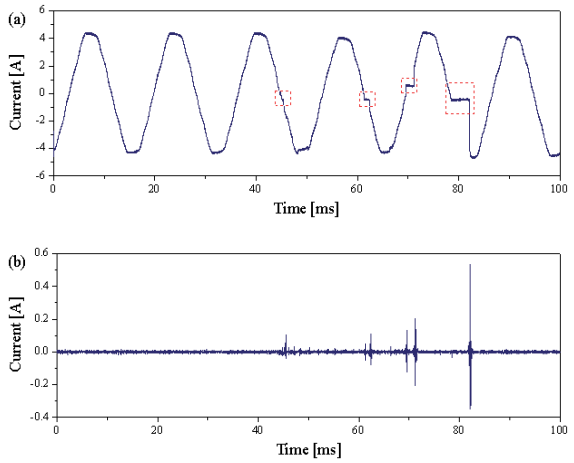

Fig. 8. Extraction of arc signal from the outlet-plug fault. (a) Mains current and (b) signal reconstructed using D6, D7, and D8.

were extracted from the terminal-cord and the outlet-plug faults. The same as that in the cord-cord fault, detail components D6, D7, and D8 were related to the arc and were used for signal reconstruction. Extraction of arc signals from the terminal-cord and the outlet-plug are shown in Fig. 7 and Fig. 8, respectively.

4. CONCLUSIONS

In this paper, the WT, which decomposes a signal into a series of independent frequency bands, was used for extracting the arc signal from the AC mains. The correlation coefficients between the single arc current pulses and the mother wavelets were calculated and the results indicated that bior1.5 had the highest similarity with the arc pulses. The signals detected from simulated arc faults including cord-cord, terminal-cord, and outlet-plug were decomposed into eight levels using the MRA method, which consistently revealed that only the components D6, D7, and D8 were related to the arc whereas other detail components D1~D5 and approximation component A8 were associated with background noise and disturbance, respectively. Therefore, D6, D7, and D8 were used for signal reconstruction. Results from this paper are expected to be applied to further analysis of arc signals in the indoor wiring system.

REFERENCES

[1] UL 1699, Arc-Fault Circuit Interrupters, 2006.
[2] I. K . Kim, D. W. Park, S. Y. Choi, C. Y. Park, H. K. Kim, and G. S. Kil, *J. Korean Inst. Electr. Electron. Mater. Eng.*, **21**, 182 (2008).
[3] G. S. Kil, K. S. Jung, D. W. Park, S. J. Kim, and J. S. Han, *J. Korean Inst. Electr. Electron. Mater. Eng.*, **23**, 554 (2010). [DOI: http://dx.doi.org/10.4313/JKEM.2010.23.7.554]
[4] C. E. Restrego, *Proc. Electrical Contacts - 2007 Proceedings of the 53rd IEEE Holm Conference on Electrical Contacts* (IEEE, Pittsburgh, PA, USA, 2007) p. 115. [DOI: http://dx.doi.org/10.1109/HOLM.2007.4318203]
[5] D. W. Park, I. K. Kim, S. Y. Choi, and G. S. Kil, *Proc. the International Conference on Condition Monitoring and Diagnosis* (Beijing, China 2009) [DOI: http://dx.doi.org/10.1109/CMD.2008.4580385]
[6] G. D. Gregory and G. W. Scott, *IEEE Trans. Ind. Appl.*, **34**, 928 (2002). [DOI: http://dx.doi.org/10.1109/28.720431]
[7] G. D. Gregory, K. Wong, and R. F. Dvorak, *IEEE Trans. Ind. Appl.*, **40**, 1006 (2004). [DOI: http://dx.doi.org/10.1109/TIA.2004.831287]
[8] S. Song, F. Wang, and G. Cheng, *Trans. Electr. Electron. Mater.*, **15**, 182 (2014). [DOI: http://dx.doi.org/10.4313/TEEM.2014.15.4.182]
[9] X. Ma, C. Zhou, and I. J. Kemp, *IEEE Trans. Dielectr. Electr. Insul.*, **9**, 446 (2002). [DOI: http://dx.doi.org/10.1109/TDEI.2002.1007709]
[10] X. Zhou, C. Zhou, and I. J. Kemp, *IEEE Trans. Dielectr. Electr. Insul.*, **12**, 586(2005). [DOI: http://dx.doi.org/10.1109/TDEI.2005.1453464]
[11] G. M. Wang, S. J. Kim, G. S. Kil, and S. W. Kim, *IEEE Trans. Dielectr. Electr. Insul.*, **24**, 200 (2017). [DOI: http://dx.doi.org/10.1109/TDEI.2016.005969]
[12] X. Ma, C. Zhou, and I. J. Kemp, *IEEE Electr. Insul. Mag.*, **18**, 37 (2002). [DOI: http://dx.doi.org/10.1109/57.995398]
[13] A. T. Carvalho, A.C.S. Lima, C.F.F.C. Cunha, and M. Petraglia, *Measurement*, **77**, 122 (2015). [DOI: http://dx.doi.org/10.1016/j.measurement.2015.07.050]
[14] I. Shim, J. J. Soraghan, and W. H. Siew, *IEEE Electr. Insul. Mag.*, **17**, 6 (2001). [DOI: http://dx.doi.org/10.1109/57.901611]
[15] C. S. Chang, J. Jin, C. Chang, T. Hoshino, M. Hanai, and N. Kobayashi, *IEEE Trans. Power Del.*, **20**, 1363 (2005). [DOI: http://dx.doi.org/10.1109/TPWRD.2004.839187]
[16] L. Satish and B. Nazneen, *IEEE Trans. Dielectr. Electr. Insul.*, **10**, 354 (2003). [DOI: http://dx.doi.org/10.1109/TDEI.2003.1194122]
[17] J. Li, T. Jiang, S. Grzybowski, and C. Cheng, *IEEE Trans. Dielectr. Electr. Insul.*, **17**, 1705 (2010). [DOI: http://dx.doi.org/10.1109/TDEI.2010.5658220]
[18] L. Yang, M. D. Judd, and C. J. Bennoch, *The 17th Annual Meeting of the IEEE Lasers and Electro-Optics Society, 2004. LEOS 2004* (IEEE, Boulder, CO, USA, 2004) p. 166. [DOI: http://dx.doi.org/10.1109/CEIDP.2004.1364215]